Achieving Impressive Global Positioning and Stability in a High Fidelity Antenna Measurement System

Jacob Kunz, Eric Kim
MI Technologies, LLC
Suwanee, GA, USA

***Abstract*—Highly accurate antenna measurements can require precise alignment and positioning of the probe antenna to the antenna under test. The positioning of the antenna during acquisition can involve the movement of several simultaneous axes of motion. This places a global positioning accuracy requirement on the positioning system. To achieve precision in global positioning and alignment, an understanding of dominant error factors such as load induced deflection/resonance, thermal deflection, positioning error sources and mechanical alignment tolerances is essential. This paper focuses on how global accuracy and stability were achieved, addressing these factors, on a recently delivered large far field antenna measurement system. The system involved eight axes of positioning with the ability to position 950 lbs. antenna under test 5.94 meters above the chamber floor achieving 0.84 mm and 0.027 degrees positioning accuracy relative to the global range coordinate system. Stability of the probe antenna after motion was within 0.076 mm.**

I. Introduction

Precise alignment and positioning of an antenna under test (AUT) with respect to a probe antenna is necessary to acquire high accuracy antenna measurements. Complex measurement acquisitions can require the movement of several simultaneous axes of motion to position the antennas with respect to each other. The specification of the alignment and positioning accuracies of the antennas to each other as achieved by multiple axes of motion is termed the global positioning accuracy. This global positioning accuracy specification limits the contribution of the positioning error to the overall RF measurement error in the system.

Many antenna measurement systems are designed and implemented as systems dedicated to the measurement of a particular antenna in a particular acquisition mode. However, maximizing facility usage sometimes requires that a system be flexible in its ability to make measurements in many different acquisition scenarios which can require different mechanical configurations. In such systems, global accuracy specification provides a means to guarantee positioning accuracy in all modes. Mechanically re-configurable systems present additional challenges in the need to implement and test precise assembly locating features that can reacquire global accuracy after disassembly and reassembly.

High accuracy positioning systems have been implemented in other measurement configurations, including radar cross section (RCS) measurements and spherical near-field (SNF) measurements. A RCS measurement positioner consisting of an overhung gantry arch and an AUT azimuth positioner achieved ±0.001° root-mean-squared (RMS) error over the two-angle scan range [1]. A SNF positioning system consisting of a 9.5-meter-radius arch and a large azimuth rotator achieved 0.204 mm RMS measurement radius error and 0.070° RMS angular pointing error natively without error correction techniques [2].

Here, a large indoor far-field (FF) measurement system consisting of a source positioner and a separate antenna-under-test (AUT) positioner is presented. The mechanical details and method of measuring and calculating the global positioning accuracy as it pertains to the antenna measurement is discussed. Major sources of positioning error and misalignments are presented along with discussions of how RF measurement strategies can improve the positioning accuracy by avoiding these sources of error. Finally, measurements and discussions of the dynamic positioning accuracy of the positioning system are presented.

II. Mechanical Design

A. Source Positioner

The source positioner is a 7-meter tall, slender structure designed to position two source horns within the test chamber. The positioner consists of a 15.85 meter linear floorslide, a custom absorber-avoiding carriage, a mast, a 1.22 meter vertical linear slide, and two high-precision roll axes as seen in Figure 1.

The linear floorslide allows the FF distance between the source and AUT to be varied from 2.40 to 18.31 meters. The floorslide is of multi-piece construction and includes full adjustability in its mounting to the floor, allowing its installation and alignment to be conducted with a high level of precision. The custom floorslide carriage is designed such that the source positioner can traverse the full floorslide length without the need to move the absorber that shadows the floorslide structure.

The mast incorporates a jog to place both the source roll axes and the floorslide rails on the chamber centerline to improve RF performance. The vertical slide at the top of the mast provides 1.22 meters of vertical travel of the vertical

carriage. The two high precision source roll axes are mounted a fixed distance apart on the vertical carriage and are aligned to provide parallel and vertically-aligned axes of rotation.

The source tower structure is designed such that the vertical slide and mast are can be removed from the chamber via the use of a single axis overhead crane. This provides full range re-configuration capabilities. Special pin-alignment features are incorporated to allow precise re-assembly with minimal loss of alignment accuracy.

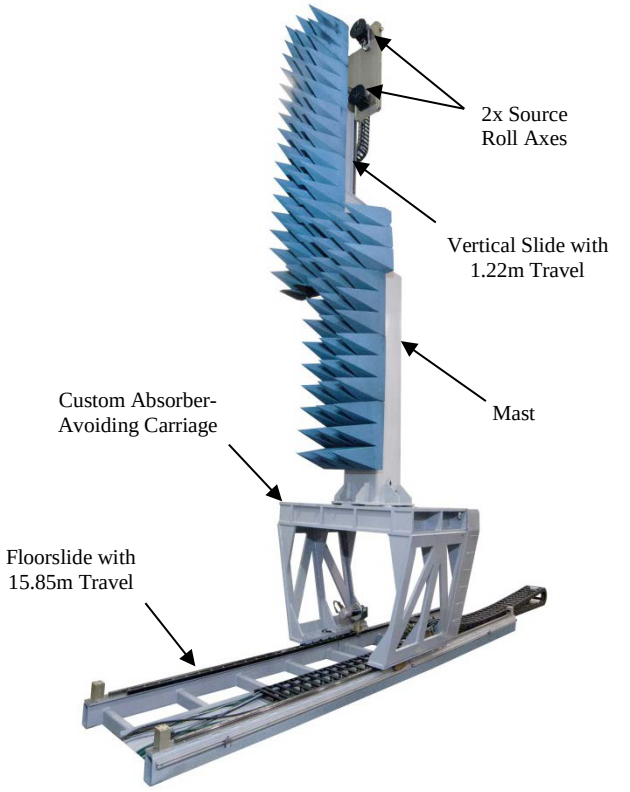

Figure 1. Source Positioner

B. AUT Positioner

The AUT positioner is a 4-axis positioner designed to provide maximum accuracy in two specific mechanical configurations, each with a specific load mass and center of gravity. The positioner consists of a lower azimuth, a motorized offset arm, an elevation axis, and an upper azimuth/roll axis as shown in Figure 2. Critical mechanical features utilized to maximize accuracy include a large lower azimuth bearing with minimal axis wobble, a highly stiff offset arm, and an elevation axis stow pin.

The AUT positioner incorporates features that allow it to operate in two distinct modes: Configuration A and Configuration B. As shown in Figure 2, Configuration A operates with the elevation axis nominally at 0° with the primary acquisition axes being the elevation and upper azimuth while the AUT aperture is at a 0.914 meter radius from the elevation axis of rotation. Configuration B uses the elevation axis stow pin to precisely hold the elevation at 90°. This allows acquisitions to be made using the lower azimuth while the upper azimuth is used as a roll axis. Additionally, a mast extension with precision alignment features is inserted between the upper positioner and the mast such that the roll axis of rotation lies on the same chamber centerline as the 0.914 meter radius antenna aperture of Configuration A.

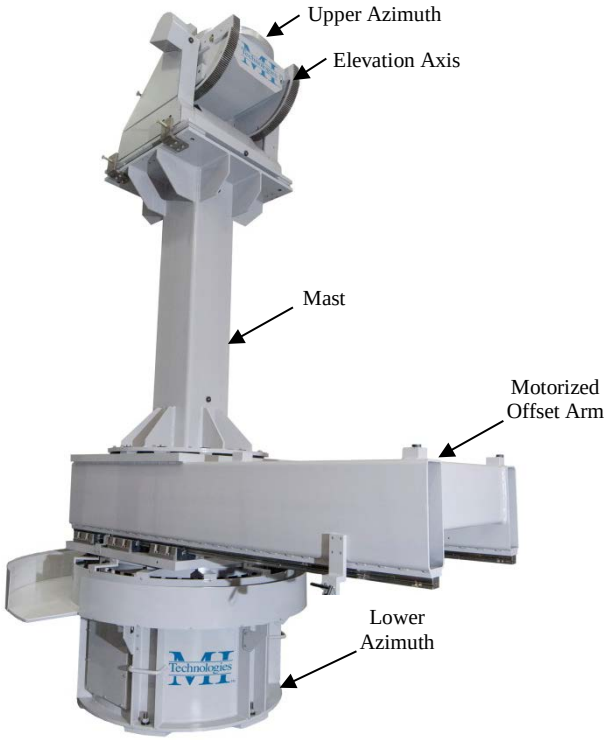

Figure 2. AUT Positioner in Configuration A

C. Motion Control

The Source Positioner and AUT Positioner are both controlled by a single MI Technologies MI-710C motion controller. The MI-710C is configured to control 8 axes with the capability to move 4 of the axes simultaneously. The motion controller serves to complete all low-level motion control including current, velocity, and position loop compensations along with higher-level control, including motion profile generation, real-time position capturing, measurement trigger generation, multi-axis coordinated motion programming, real-time position error correction, and emergency stop implementation.

The coordinated motion capabilities of this controller provide the ability to program arbitrary motion relationships between up to the 4 simultaneous axes available in this configuration. This feature allows a drastic reduction of measurement acquisition time and eliminates some data post-processing by eliminating such hindrances as duplicate sampling and positioning parallax.

The system requirements of high accuracy during dynamic motion measurements and high-fidelity coordinated motion are a challenge given the non-linearities of varying mechanical loadings and multiple mechanical configurations. The MI-710C motion controller overcomes these challenges by utilizing multiple tuning profiles on each axis, which can be tailored to

particular operating conditions. The measurement system instruction set needs only to select the appropriate pre-programmed profile for the required test scenario.

III. Global Accuracy Measurement

A. Global Accuracy from Component Measurements

Commonly, individual mechanical positioners are designed and tested as standard products to meet specified native positioning accuracies on their axis/axes of travel which only accounts for 1 or 2 degrees-of-freedom (DOF). These catalog specifications often do not include positioning accuracies in the non-actuated directions which leaves open-ended assumptions of zero positioning error in the remaining 4 or 5 DOF. Additionally, specifications are guaranteed in an unloaded condition as accuracies vary with the load which is unknown to a standard product. The goal of global accuracy specification is to capture the overall accuracy in 6-DOF in the presence of the actual antenna loads, thereby limiting the positioning-induced RF error in the final measurement system.

The specification of the global accuracy of this system is simplified by limiting it to the global accuracy in the three dimensions most relevant to the far-field RF measurements being made. Figure 3 shows the complete far-field positioning system, which uses the AUT positioner to orient the AUT and uses the source positioner to locate the source at the desired separation distance and bore sight position. The three dimensions scrutinized by the global accuracy specifications of this system are the AUT azimuth and elevation pointing errors to the source aperture and the separation distance from the source antenna aperture and the AUT aperture.

Figure 3. Far-Field Position System

The global accuracy specification of the system needs to encompass all mechanical configurations, load conditions, axis travel ranges, and motions utilized during measurements. Proving such a specification through measurement would have a very large experimental domain if every factor combination was tested. An alternative approach is taken by limiting the test set such that the accuracy across the domain of each factor is measured at a single set point of the other factors. This limits the number of tests to match the number of factors of interest. The accuracy measurement across each factor is then combined to provide an estimate of the global accuracy. Combining the individual errors from each factor relies on the assumption that the error contribution of each factor is independent of that from the other factors. Independence of the factors allows the total error to be estimated by a root-sum-square (RSS) of the individual factor RMS errors as shown in (1) where e_i is the RMS error for individual factor test i and E_{total} is overall RSS error.

$$E_{\text{total}} = \sqrt{\sum \left(e_i^2 \right)} \tag{1}$$

B. Component Measurement Details

The individual accuracy tests were developed to capture the individual contributions of each axis to the overall global error. These tests, detailed in Table I, examine subsets of motion of the system which were deemed to be the largest contributors to overall AUT pointing and separation error relative to the RF source. Tests of the AUT upper positioner are conducted in both Configuration A and B. The final test is the measurement of the nominal alignment error of the two positioners to each other. This error is added to each of the other test error results.

TABLE I. Component Accuracy Measurement Tests

Test #	Actuated Axis	Condition
1	AUT Az and AUT Roll	Configuration A
2	AUT Az and AUT El	Configuration B
3	AUT Offset	Configuration A
4	Source Floorslide	
5	Source Vertical Slide	
6	Source Roll	
7	Offset Stability	Configuration A
8	Floorslide Stability	
9	Vertical Slide Stability	
-	Nominal Alignment Error	Configuration A and B

C. Test Equipment and Methodology

The measurement of positioning accuracy incorporates the use of an API Radian laser tracker metrology system. These systems are widely used in the RF measurement industry along with many other industries to precisely measure 3D positions in large scale devices. The laser tracker operates by utilizing a high-precision, automated tracking head for motion and laser pointing direction measurement and using optical methods with the laser to measure target distance. The target, which the laser tracker measures, is a spherically mounted retroreflector (SMR) which can be placed anywhere in the working volume for a measurement as long as the laser head maintains line-of-sight of the target.

Measurement of a single SMR target provides a 3D location within the global coordinate system, but it does not provide any information on the attitude of the target. Acquiring this information requires the use of three targets which are rigidly mounted on an SMR fixture such as that shown in Figure 4. Measuring all three targets provides a planar triangle object. The three targets can be re-measured after movement has occurred and the planar triangle can be re-acquired. Assuming that the fixture is rigid, the shape of the planar triangle would be the same, but its location and orientation would be different. The change in location and orientation of the 3-SMR constellation is what is compared to the controller readout positions to calculate positioning errors.

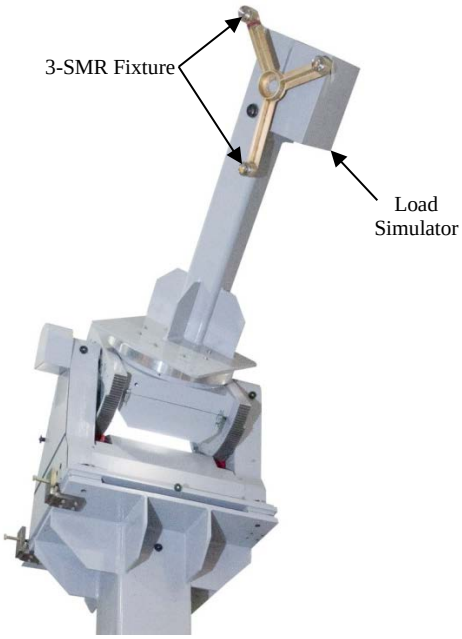

Figure 4. Test Article Simulator with SMR Fixture

Use of the laser tracker and 3-SMR constellation requires best practices that can be implemented to improve the fidelity of the measurements. First, the 3-SMR constellation should form a triangle in which all three sides are different lengths. This will eliminate singularities in the calculated changes in position and orientation. Strategy in laser placement with respect to the view of the three SMRs across the full range of an axis' motion is important. The SMRs have a limited angle at which they can accept the laser light. This means as the positioner moves, the target SMRs must be counter-rotated in order to continuously point at the laser tracker. Each counter-rotation action risks inducing unknown errors into the SMR's measured position. Additionally, use of the laser tracker system for high accuracy measurements requires extreme care and knowledge of its operation leading to precise control of such factors as environment and part temperature, air particulate content, tracker stand stability, global coordinate constellation implementation, and numerical computation algorithms. Oversight in any of these critical variables can lead to inaccurate measurements in a manner that is often undetected.

IV. Static Global Accuracy Results

The process of assembling and aligning a multi-axis positioning system involves not only placing the axes where desired in the test chamber, but also aligning the axes of motion to one another with the goal of perfect perpendicularity, parallelism, and axis intersections where appropriate. However, there is a specific configuration where all of these errors are minimized and that configuration needs to correspond with the center of measurement travel during the most used/highest priority test scenario. All measured global positioning errors are then represented as error deviations from this initial position. The alignment errors at this initial position are then added to the measured error deviations to provide the global errors for each axis.

A. Source Tower Error Measurements

Measurement of the global error caused by motion of the source tower along the 15.85 meter floorslide showed that it was the largest single contributor to FF azimuth pointing error and FF separation error. The source of these errors resides in the geometric relationship between the footprint of the floorslide carriage and the height of the tower. The floorslide carriage has an approximate 1 meter square footprint while the tower is 7 meter tall at the source antenna's highest aperture position. This ratio of 7:1 means that any horizontal flatness or straightness deviation in the floorslide rails is amplified to a 7x deviation at the top of the tower. For example, if one of the two rails has a section that is 0.005" taller than the other rail, then the entire tower will roll to the side causing the top of it to deviate 0.035" sideways from the chamber centerline. At positions close to the AUT positioner, the small separation distance causes these sideways displacements of the source to manifest as large azimuth angle error between the AUT and source antenna. Similarly, high spots in both the rails can cause the tower to pitch forwards and backwards resulting in separation distance errors that are not captured by the position feedback transducer on the floorslide rail.

The vertical slide made minor contributions to the overall positioning error in the system. While it has the same mechanical setup as the floorslide with two bearing rails, the relationship between the vertical slide carriage footprint and the distance to source horn aperture is much more favorable with a 1:1 ratio such that rail straightness errors are not amplified.

The source roll stages are high precision and are composed of dual high stiffness bearings separated by a large distance given them very stable axial motion. This, combined with the fact they are the last positioners in the stackup, caused their error contribution to be two orders of magnitude smaller than that of other axes.

B. AUT Positioner Error Contributions

The AUT lower azimuth axis is only utilized in Configuration B of the FF measurements. Its contribution to the global axis error, mostly impacted the separation distance accuracy of the range. The source of this is the relationship between the bearing footprint and the height of the AUT positioner. The weight of the AUT positioner stackup causes the lower azimuth bearing and housing to deflect as it rotates. The relationship between the 1 meter diameter lower azimuth

and the 5.5 meter tall AUT stackup causes these small deflections to be amplified 5.5x at the top of the AUT positioner. It is worth noting however, that the angular RMS errors caused by the lower azimuth are approximately the same as its max/min native accuracy unloaded.

The AUT offset arm is the largest error contributor to the AUT global elevation error. The large weight of the AUT positioner mast and upper positioner causes the arm to undergo overhung-beam deflection as the offset distance is increased resulting in an AUT elevation pointing error. This behavior is only troubling in measurement scenarios where the offset arm is moving during different points in the measurement. Most measurement acquisitions will setup with the offset arm in a single position at which point electrical bore sighting operations using the AUT elevation axis would remove the error. As long as the offset arm and AUT elevation axis remain at these positions, the removed error would not deviate throughout the test.

The AUT elevation axis is only utilized in Configuration A. Measurement of its accuracy showed that its greatest error contribution was in the global AUT elevation pointing error. While this error occurs when the AUT elevation axis is actuated, it is actually again caused by the offset arm. Since the radius between the AUT elevation axis of rotation and the AUT center of mass is almost 1 meter, moving the elevation axis through it full range of motion causes a large variation in moment loading of the offset arm. The large change in moment loading results in a large variation of offset arm deflection and therefore a large variation in AUT elevation pointing error.

The AUT roll/azimuth axis contributed relatively small positioning error to the overall system. This is similar to the source roll axes because these axes are the closest link to the measurement target and have minimal geometric amplification of the errors.

C. Computed Static Global Accuracies

A summary of final global accuracy values computed from the combination of the individual measurements is shown in Table II. It is observed that over all of the mechanical configurations and travel ranges, the RMS pointing accuracy of the AUT to the source is 0.011° in azimuth and 0.027° in elevation. Additionally, the RMS separation distance accuracy of the far field positioning system is 0.036 inches.

TABLE II. COMPUTED STATIC GLOBAL ACCURACIES

Actuated Axis	Condition	RMS Accuracy
Far Field Azimuth Angle	Configuration A	0.010°
	Configuration B	0.011°
Far Field Elevation Angle	Configuration A	0.027°
	Configuration B	0.024°
Far Field Separation Distance	Configuration A	0.036”
	Configuration B	0.033”

Positioning systems that are specified by their global accuracy require the end users to have explicit knowledge of the positioning error measurement tests and physical setup to quantify the impact on RF measurements and minimize the effects. For example, the RMS global accuracies are errors between the controller reported position and the actual pointing errors and distance between the axes-of-rotation. Setup of an AUT requires either precise mechanical alignment between those axes and the RF wavefront or electrical bore sighting operations need to be performed to offset the axis positions to operate about the true bore sight pointing direction.

Additionally, most of the global error is caused by specific travel ranges of only a few of the axes. RF measurements that limit the motion of those axes will achieve significantly better global accuracies. Simple measurement strategies can be implemented to further reduce the mechanical position errors.

V. DYNAMIC POSITIONING ACCURACY

A. Contribution of Vibration to Global Error

The global positioning errors presented thus far comprise of static position readout errors. From an RF measurement perspective, this corresponds to a fully stepped-motion acquisition with significant dwell times between the stopping of the motion and the moment at which RF data is captured. That is the only way to achieve those positioning error values without specifically characterizing the dynamic positioning errors in the system.

However, RF measurements are conducted in step-scan acquisition modes in which RF data is captured while one or more axis are continuously moving. During axis motion, vibration of the mechanical structure can be excited through various phenomena, including momentum loading during trajectory accelerations, torque cycling from gear meshes and torque variations due to control loop cycling. Some mechanical vibrations, such as some scenarios of gear loading variations, are captured within the actual axis position encoder since on-axis encoders are used throughout this system. However, most vibrations create motion, such that the actual positions of the AUT or source horn are displaced from their static location at that particular readout position.

The largest contributor to vibration excitation is the momentum loading caused during axis acceleration and deceleration. The motion will primarily excite vibration in its direction travel, but there could be cross-coupling of stiffness between orthogonal directions within the positioner. This cross-coupling could, for example, create vibration in the cross-range direction, even though the axis travel direction is acting to primarily excite vibration in the vertical direction.

B. Vibration Mitigation

The most effective and robust method of mitigating vibration in a positioning system is through careful mechanical design to maximize stiffness in the primary directions of motion. The far field source tower in this study maximizes its floorslide carriage stiffness in the chamber centerline direction because it is the primary direction of motion of the floorslide. Though the carriage is an order of magnitude more compliant in the cross-range direction, motion did not exhibit any significant vibration in that direction due to both the lack of primary movement in that direction and to the lack of stiffness coupling in the orthogonal directions of the carriage.

While improved mechanical stiffness serves to address vibration from the control system plant, the controller design addressed the vibration mitigation through the excitation input

side. This system utilized state-of-the-art s-curve motion profiles to avoid broad-band dynamic excitation of the positioner natural frequencies [3].

C. Vibration Measurement

The vibration excited by movement was measured during actuation of individual axes. During these tests, the laser tracker continuously measured a single SMR target using a hardware trigger generated by the motion controller. The hardware trigger implementation allows the controller readout position to be synchronized with the laser measurements in order to calculate true readout error during the vibration. This test only provides 3-DOF position data as multiple SMRs cannot be measured simultaneously.

Figure 5 shows the position of the source antenna as measured by the laser tracker while the floorslide is commanded to make a 254 mm (10 inch) step motion. The RF measurement system commences measurement after the motion controller has reported that is motion is complete. It is desired that the residual vibration after that point does not introduce any position error when compared to the readout position of the controller.

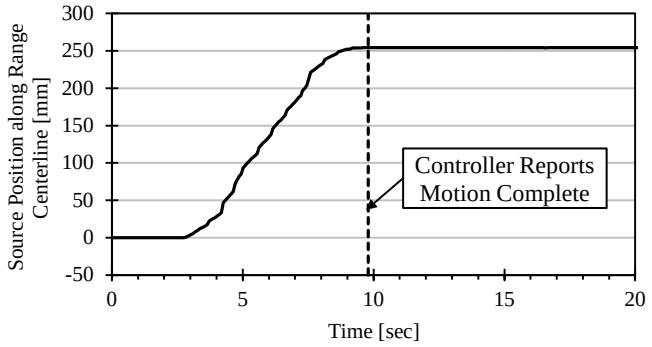

Figure 5. Measured Source Motion as Floorslide Traverses along Range Centerline

Figure 6 shows a detailed view of the residual motion after the floorslide motion is complete. Key features to notice are the steady-state error of around 0.080 mm and the large movements that occurred around 16-18 seconds. The steady-state error could be attributed to either the control loop steady-state error or it could be caused by actual position readout error. The large movements are caused by the control loop either attempting to correct for the final steady-state error or reacting to a system disturbance such as a vibration force.

The use of the hardware triggering of the laser along with triggering the position capture feature of the motion controller allows the readout position of the axis to be subtracted from the measured position. The results of this operation, shown in Figure 7, provide the actual position readout error immediately after the controller indicates motion is done. It is seen that the residual vibration in the axis attributes a maximum error 0.040 mm.

Similar measurements were made on all of the motion axes. Overall, it was determined that error contribution from mechanical vibrations did not exceed 0.076 mm in separation or 0.002° in azimuth and elevation angles.

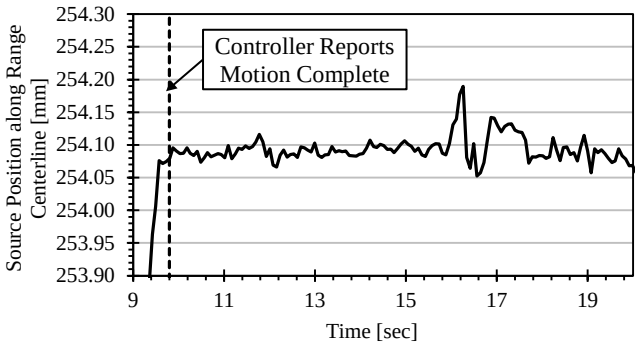

Figure 6. Raw Measured Source Motion after Controller indicates Motion is Complete

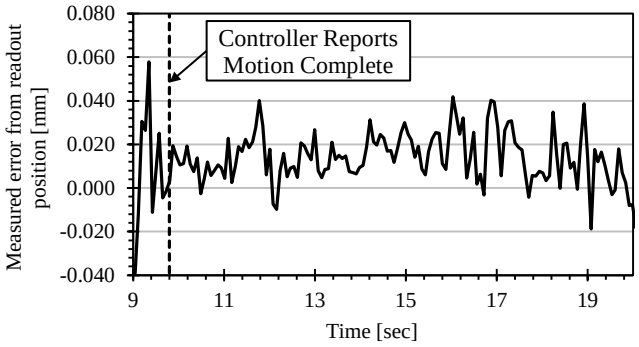

Figure 7. Measured Position Error from Controller Readout Position

VI. Conclusions

The far-field positioning system presented provided more than sufficient global accuracy to meet the antenna measurement requirements. The mechanical design of the positioner proved to provide sufficient positioning accuracy and dynamic stiffness to pass all accuracy specifications. The global accuracy measurement method proved to provide sufficient qualification of the overall global accuracy across all axes' range of travel and mechanical configurations while minimizing the length and number of accuracy measurements needed. The accuracy measurements showed that the largest positioning errors were contributed by the floorslide and offset arm which are setup axes in most measurement scenarios providing the potential to not always be factors. The overall measured RMS errors were 0.914 mm, 0.011° in azimuth and 0.027° in elevation. Measurement of the dynamic accuracy of the positioners showed that no residual vibrations contributed more than 0.076 mm and 0.002° of AUT azimuth and elevation error.

References

[1] P. Massaloux, P. Bérisset, "Achieved mechanical Accuracy of a 3D RCCS spherical near field Arch Positioning System", AMTA, 2012.

[2] S. McBride, et. al., "A Large Spherical Near-Field Arch Scanner for Characterizing Low-Frequency Phased Arrays," AMTA, 2010.

[3] Pinson, Charles, "Improved Coordinated Motion Control for Antenna Measurement," AMTA, 2012.